Developing novel fibres for endoscopic imaging and sensing

Developing Novel Fibres for Endoscopic Imaging and Sensing

Stephanos Yerolatsitis[1,*], Harry C. Wood[1], Fei Yu[2], Michael G. Tanner[3], Sarah McAughtrie[4], Holly Fleming[4], Colin J. Campbell[4], Tim A. Birks[1], Jonathan C. Knight[1], and James M. Stone[1]

[1]*Department of Physics, University of Bath, Bath, UK*

[2]*R&D Center of High Power Laser Components, Shanghai Institute of Optics and Fine Mechanics, Chinese Academy of Sciences, Shanghai, China*

[3]*Scottish Universities Physics Alliance (SUPA), Inst. of Photonics and Quantum Sciences (IPaQS), Heriot-Watt University, Edinburgh, UK*

[4]*School of Chemistry, University of Edinburgh, Edinburgh, UK*

* *e-mail: s.yerolatsitis@gmail.com*

ABSTRACT

We are developing the next generation of optical fibres for endoscopic imaging and sensing. Our imaging fibre bundle is fabricated from OM1 PCVD graded index preforms made for the telecommunications market. Whilst having a lower numerical aperture, the performance of the imaging fibre is shown to be comparable to the current state-of-the-art commercial microendoscopy fibres. In addition, we are developing negative-curvature optical fibres, which exhibit ultra-low silica Raman background. Measuring Raman spectra through an optical fibre is usually complicated by the high intrinsic Raman scatter of the fibre material. Common solutions such as the use of multiple fibres and distal optics are complex and bulky. The single hollow core negative curvature fibre is used for Raman and surface-enhanced Raman spectroscopy sensing with no distal optics while showing a 1000x background reduction compared to conventional fibres.

Keywords: endoscopic imaging, Raman spectroscopy, optical fibres.

1. INTRODUCTION

Single-use compact fibres are desired for endoscopic use. Such fibres can provide an alternative non-invasive solution for tissue diagnosis. For imaging fibres, an obvious way to produce cost effective single use imaging fibres is to use preforms made for the telecommunications industry. The main challenge is to overcome the performance limitations imposed by the choice of these starting materials to produce a high-quality imaging fibre. In conventional endoscopic imaging systems, an imaging fibre is formed of many thousands of cores. Each of the cores in the imaging fibre acts as a pixel to transmit part of an image down the length of the fibre which can be analysed in real time at the proximal end. For high-resolution images, the individual cores of the imaging fibre need to be as close together as possible. However, the core-to-core coupling limits the minimum spacing of the cores and therefore the resolution of the fibre. The cross-coupling becomes worse if the refractive index contrast of the cores is low (i.e. in telecommunications preforms), the size of the cores is small compared to the wavelength of the transmitted light or if the cores are similar in size [1]. There is a variety of techniques used to suppress coupling [2-3]. Our technique involves multi-stacking arrays of different sized cores such that no two adjacent cores are the same size. In such a way, we can minimise the coupling between cores, enabling us to use a single low-cost multimode telecommunication preform as a starting point.

In addition, developing compact sensing fibres for fibre-fed Raman systems is also challenging. When light from a spectrally narrow pump passes through a fibre, a Raman signal is generated by the silica glass. This background signal is large enough to overwhelm any signal collected from the biological sample of interest at the distal end of the system. For that reason, such systems use different fibres for excitation and collection, spatially separating the background signal from the collected signal. This is problematic because the two fibres do not physically point at the same position and distal optics are required to correct for this [4]. When working in endoscopic systems, for example in the distal lung, additional optics and filters cannot be accommodated.

To overcome this, we use a hollow core negative curvature fibre (NCF) to transmit the pump and collect the signal from the distal end. Its mode is guided in air and therefore interacts very little (10^{-4} mode field overlap) with the silica [5], greatly reducing the silica background. The silica background was an order of magnitude lower than previously reported [6], and over $1000\times$ lower from a solid-core fibre. Because of the simplified structure, the light in a NCF interacts less with the silica than in other HCFs [6, 7]. By carefully designing the fibre we managed to achieve a similar collection efficiency to that obtained by pumping via a solid fibre, allowing the measurements of weak Raman signals that overlap spectrally with the silica background.

2. LOW INDEX CONTRAST IMAGING FIBRE

The imaging fibre was formed from a commercial preform manufactured for telecoms applications. It had a graded index Ge-doped core and a thin pure silica cladding. The core-cladding diameter ratio of the preform was 0.74 with a peak refractive index contrast corresponding to a numerical aperture (NA) of 0.3. The stack and draw method was used and a stable square stack from rods drawn to different outer diameters was created from

the same preform. The fabrication method uses N different sized elements stacked in an $N \times N$ array to form a uniform square element. The uniform square element is then stacked multiple times to build up a large array of cores. The stacked squares can easily be drawn down again and restacked in order to easily build up very large arrays, as shown in Fig. 1. For this demonstration, a 5×5 array of 5 different rod sizes (2.23 mm, 2.52 mm, 2.74 mm, 2.95 mm and 3.17 mm) was stacked in a square stacking jig such that each size only appears in each row or column once (Fig. 1a). The stack was drawn down to 2.5 mm sided squares., forming the unit element for the next step of the process. The unit squares were restacked with the same orientation in a 6×6 array (Fig. 1b). This stack was drawn to 4.5 mm sided squares and restacked in a 3×3 array. The final stack was placed into a jacket tube with pure silica packing rods around the outside and drawn to canes under a vacuum to remove the interstitial gaps. Finally, the canes were drawn to a fibre with 8,100 cores in total (Fig. 1c). The outer diameter of the fibre was 550 μm with an imaging square size of 450 μm along the diagonal. The core diameters in the fibre were between $2-3$ μm with $3-4$ μm centre to centre separations depending on the particular pairs of core sizes.
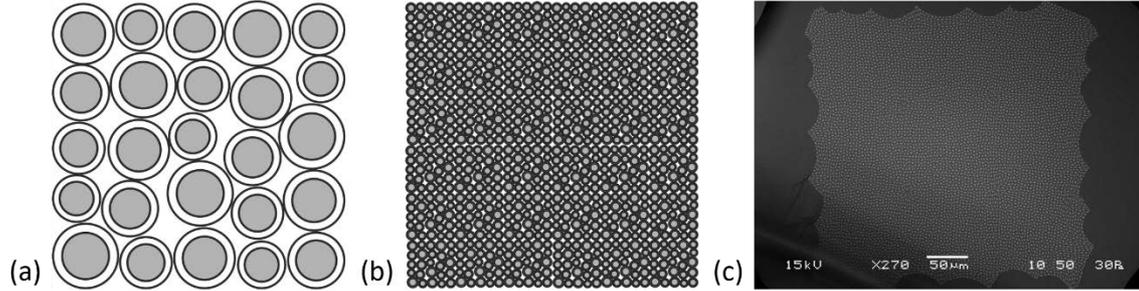

Figure 1: (a) A representation of the initial stack (grey indicates the Ge-doped core regions and white the pure silica regions); (b) The second stacking stage of our process; (c) An SEM image of the final fibre.

To compare the performance of our fibre to a commercially available fibre, a fluorescence imaging system was built and images of a 1951 USAF test target were acquired. By obtaining test target images at different wavelengths, the resolution of our fibre for these wavelengths was determined. A supercontinuum source filtered to two excitation bands (420 nm – 510 nm and 600 nm – 650 nm) was used as a light source. The filtered excitation light passed through a dichroic beam splitter and was coupled into our fibre through an aspheric lens with an NA of 0.5. The USAF 1951 targets were imaged at zero working distance from the distal end of the fibre with either a green fluorescent or red fluorescent slide placed behind them. Light emerging back out of the proximal end of the fibre was imaged onto a CCD camera (Fig. 2) after passing through the dichroic beam splitter and a second collection filter with two wavelength bands, 520 nm – 600 nm (green band) and 650 nm – 750 nm (red band).
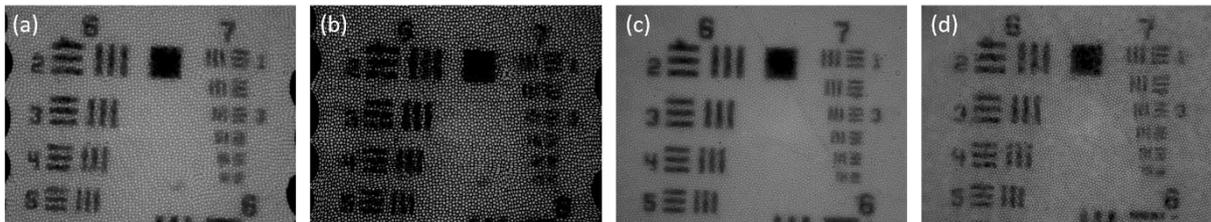

Figure 2. USAF 1951 test target fluorescent images taken through a 90 cm piece of our fibre (at (a) 520 – 600 nm and (b) 650 – 750 nm) and a commercial fibre from Fujikura Ltd. (FGIH-30-650s) (at (c) 520 – 600 nm and (d) 650 -750 nm).

In the green band image (Fig. 2a), in our fibre, several of the larger elements of group 7 are discernible down to element 3. (The elements have line widths of 3.10 μm.) These are comparable sizes to the core to core separations, indicating that very little light is coupled from one core to another. In the red band (Fig. 2b) the image contrast is degraded due to the core to core coupling. However, in our fibre, the larger elements of group 7 are still discernible down to element 2 although with reduced clarity compared to the images taken in the green band. The performance of our fibre (Fig. 2a and 2b) is still comparable to a commercial fibre (Fig. 2c and 2d) with higher numerical aperture cores.

3. NEGATIVE CURVATURE ANTIRESONANT HOLLOW-CORE FIBRE

The NCF (Fig. 3a) was fabricated using the stack-and-draw technique. The inner region consists of a ring of 6 silica capillaries around the hollow core. The thin walls of the capillaries act as resonators, confining the light in the hollow core at anti-resonant wavelengths [5]. Surrounding this region is an additional ring of 8 multimode

cores made from solid Ge-doped silica, designed to collect the Raman signal from the distal sample. The NA of these cores is 0.3 and their diameter is 28 µm. The outer diameter is 210 µm. The 20 µm hollow core is designed to guide light at 785 nm. The experimental setup is shown in Fig. 3b. Light from a fibre-pigtailed 785 nm diode laser was coupled to the proximal end of 1 m of the NCF via a bandpass filter (to remove silica background from the pigtail fibre) and a dichroic mirror (to separate any Raman signal from the pump). A long-pass filter in the collection arm filters out any residual pump. A 100 µm core graded-index multimode fibre (NA = 0.3) was used to collect the returned light from the entire proximal end-face of the NCF and deliver it to the fibre-coupled spectrometer.
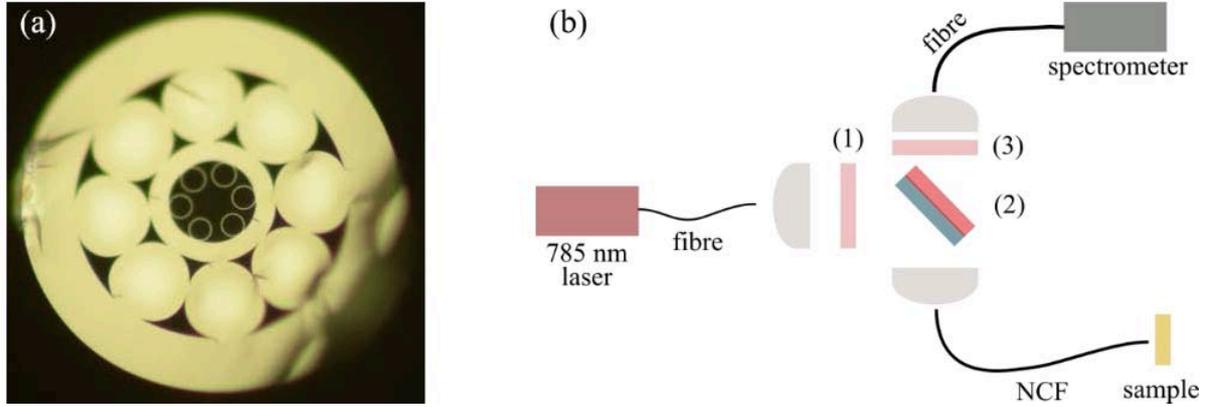

Figure 3: (a) Optical micrograph of the NCF. The outer diameter of the fibre is 210 µm, and the hollow core diameter is 20 µm; (b) Experimental setup where (1) is a 785 nm band-pass filter (2) is a 785 nm dichroic mirror and (3) is a 791.6 nm long-pass filter.

To demonstrate the reduction of silica background, the Raman response of the system was measured with pump light in the hollow core without any sample at the distal end of the fibre, Fig. 4a. To compare this with the performance of a solid-core fibre, we simply coupled the pump light into one of the Ge-doped collection cores instead of the hollow core and repeated the measurement. Figure 4 shows the Raman response of the hollow core (a) and the Ge-doped core (b). There is a 1000× reduction of the silica background when the pump light was coupled to the hollow core compared to the solid core. Indeed, a $10^5×$ reduction is possible in theory, given by the overlap of an NCF mode with the glass [5], though this would require a perfect match with the mode of the pump fibre.
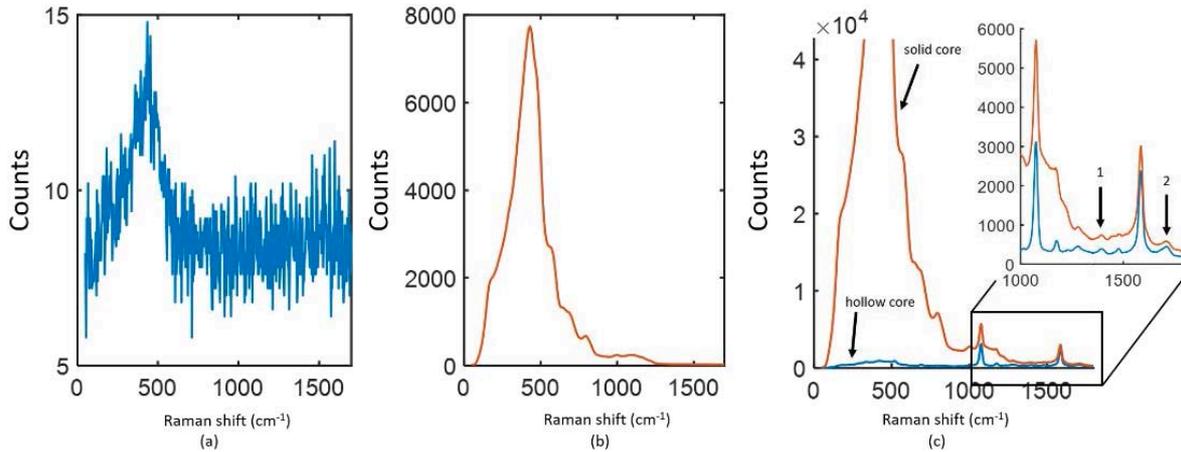

Figure 4. Generated silica background when pump light was coupled to: (a) the hollow core (blue) and (b) the solid core (orange) (1 s integration time); (c) The SERS signal from the sample collected when pumped via the hollow core (blue) and the solid core (orange), 1 and 2 are the MBA Raman peaks used for pH sensing (10 s integration time).

We then placed a SERS sample at the distal end of the NCF and recorded the Raman spectrum when pumped via the hollow core and one of the solid collection cores in turn. The sample comprised paramercaptobenzoic acid (pMBA) labelled gold nanoparticles deposited on a gold-coated microscope slide. Fig. 4c shows the collected signals, which match the published spectrum of MBA [8]. The peaks around 1050 cm^{-1} and 1550 cm^{-1} have similar heights in both cases, indicating that the collection efficiency is similar when pumped via the solid core and the hollow core, whereas the background is much reduced when pumped via the hollow core. MBA can

be used for pH sensing [8] by measurement of the ratio between the intensity of the two small peaks (labelled 1 and 2) around 1380 cm^{-1} and 1700 cm^{-1}. Eliminating the silica background through the use of the NCF should improve the accuracy of this measurement [8]. We have also demonstrated the use of this setup for measuring the intrinsic Raman response of ethylene glycol.

4. CONCLUSIONS

We demonstrated the fabrication of two novel fibres, an imaging and a Raman sensing fibre. The performance of the imaging fibre is shown to be comparable to the current state-of-the-art commercial products, whilst using standard starting materials shared with the telecommunications industry. This technique should allow cost-effective, single use fibres for endoscopy to be fabricated. In addition, we have demonstrated the use of NCF for Raman sensing. The generated silica background is an order of magnitude smaller compared to other schemes [6,7] while maintaining the same collection efficiency as a solid fibre. This was achieved without the use of any distal optics or any additional fibres.

ACKNOWLEDGEMENTS

REFERENCES

[1] A. W. Snyder and J. D. Love: *Optical Waveguide Theory*, Kluwer Academic Publishers, p. 387, 1983.
[2] Schott North America: *An Introduction to Fiber Optic Imaging*, Schott, 2007.
[3] http://www.us.schott.com/lightingimaging/english/medical/medical-products/transmitting-images_leached-image-bundle.html
[4] J. T. Motz *et al*.: Optical fiber probe for biomedical Raman spectroscopy, *Appl. Opt.* vol. 43, pp. 542-554, 2004.
[5] F. Yu and J. C. Knight: Negative curvature hollow-core optical fiber, *IEEE J. Sel. Topics Quantum Electron.*, vol. 22, pp. 146-155, 2016.
[6] P. Ghenuche *et al*.: Kagome hollow-core photonic crystal fiber probe for Raman spectroscopy, *Opt. Lett.* vol. 37, pp. 4371-4373, 2012.
[7] S. O. Konorov *et al*.: Hollow-core photonic crystal fiber-optic probes for Raman spectroscopy, *Opt. Lett.* vol. 31, pp. 1911-1913, 2006.
[8] D. Choudhury *et al*.: Endoscopic sensing of alveolar pH, *Biomed. Opt. Express*, vol. 8, pp. 243-259, 2017.